New Experimental Evidences of Anomalous Forces in Free Fall Locked Magnets

Preprint · May 2021

DOI: 10.13140/RG.2.2.30898.32968

2 authors:

Elio Battista Porcelli
H4D Scientific Research Laboratory

Victo S. Filho
H4D Scientific Research Laboratory

New Experimental Evidences of Anomalous Forces in Free Fall Locked Magnets

Elio B. Porcelli[1,*] and Victo S. Filho[1]

[1]H4D Scientific Research Laboratory, 04674-225, São Paulo, SP, Brazil

*Correspondence: elioporcelli@h4dscientific.com

Abstract

In this work, we measured the magnitude of forces raised in the free fall of high magnetic field coupled magnets. By using a high accurate accelerometer connected to the falling magnets we measured unexpected and weak decreasing or increasing in the local gravity acceleration which has no traditional explanation, indicating the possible influence of quantum mechanisms as responsible by the anomalous effect. We also propose a simple model based on the generalized quantum entanglement hypothesis which applied to that physical system provides us the magnitude of such a macroscopic force as originated by the microscopic magnetic dipoles constituting the magnets. The new results corroborated the positive results of previous experiments and are consistent with the validity of our theoretical forecast.

Keywords: high magnetic field magnets; magnetic dipole forces; quantum entanglement; anomalous forces

1. Introduction

1.1 Outline of the Phenomenon

Some simple experiments in which repulsive conjoined magnets fell freely showed that Galileo's traditional experiment was challenged in the sense that the coupled magnets were slower than any another ordinary object with the same weight and similar shape. According to Galileo, two objects must fall with the same acceleration if they are simultaneously released at same height. On the other hand, attractive conjoined pair magnets would fall faster than any another equivalent ordinary object. Those runs were inspired by the researcher Boyd Bushman at Lockheed Martin Tactical Aircraft Systems, who proposed a device simulating a magnetic monopole responsible for generating a beam which could emit pulses and levitate, among other applications [1]. In a 2003 interview[2], Boyd Bushman claimed that if one dropped two locked magnets with opposing magnetic poles (inversely aligned), the opposing magnetic forces would affect the gravity field of the Earth such that the body would fall slower than if the poles were aligned. In the interview, Bushman asserted to have realized 500 experiments of free falls from a height of 59 feet and verified the effect cited by him. In 2009 William Alek performed a magnet drop experiment where he claimed to have positively replicated Boyds finding[2]. He had received criticism due to the realization of one unique test and for releasing the magnets by hand rather than with a trap door mechanism. Despite the clear need for such experiments to be improved, they reinforced evidences of forces involving the so called non-local interactions between magnetic dipoles of the magnets and the planet such as already emphasized in other previous works related to magnetic cores and gyroscopes[3, 4].

This fact encouraged us to perform our own experiments related to magnets free fall, having in mind that the experimental setup for that should address a more significant enhancement in the effect so that it was really doubtless verified. In fact, one aims to investigate if the effect does exist and it is not due to noises, electrostatic or any other possible interference. For achieving such a main objective we implemented an innovation which consists in using a high resolution accelerometer coupled to the devices, so that a big quantity of data was collected at all instants of the falls. We detail our experimental work in next section. Beside our experimental investigation, we also intended to understand the theoretical mechanism for the effect. Our previous works involving magnetic cores [3] and gyroscopes [4] remarked that the transition of atomic magnetic dipoles over magnetic fields (local interactions) can non-locally interact with the outer particles of the planet, considering the preexisting condition of generalized quantum entanglement between all particles. So, we also suppose that the collective transition of the myriad of dipoles can responsible by the so called anomalous forces measured in the experiments also resulting in variation of the weight (reaction force) of the magnetic devices. In summary, in this work our main objectives are to measure significant and magnitudes of such forces and construct a theoretical model based on our GQE hypothesis aiming to explain in a consistent way the experimental results obtained.

In next sections, this work describes our experimental setup and reports the new measurements of force obtained from that configuration. In the following, we present our theoretical model in order to present a consistent explanation for the phenomenon. Finally, in the last section we discuss our conclusions and final remarks.

2. Experimental Works

2.1 Previous Experiments

Our experimental work involved two possible configurations: the free fall of conjoined magnets when both of them suffer a repulsive force and the free fall of them when the force between them is attractive. In case of two inversely conjoined magnets (in which there is the repulsive force between them), the magnetic field lines are divergent, so that their internal dipoles point out in omnidirectional way. As the result, a reaction force can be taken place in the same way than gravity force direction. The magnets can suffer an increasing of the free fall acceleration.

Some simple experiments [5, 6, 7] involving inversely (repulsion) and attractive conjoined magnets reported that they fell respectively slower and faster than an ordinary equivalent object released in the same height and same time. Another simple experiment [8] reported that inversely conjoined magnets fell slower than other ordinary object with the same weight and shape. According to the authors of those experiments, such runs confirmed the experiments of the researcher Boyd Bushman [2] to who it is attributed the pioneer works in this study.

Such results motivated us to investigate the phenomenon by means of our own experiments, which we describe in the next section.

2.2 Our Experimental Setup

Our experiment consisted in performing free falls of two cylindrical magnets under attraction (setup 1) and also of two cylindrical magnets under repulsion (setup 2), as shown in the experimental setup drawn in figure 1. In the figure 2, we show a photo of the experimental setup used in our free fall experiments for both cases of conjoined magnets. We also implemented the free fall of non-magnetic materials (quartz crystals) for comparison with the two setups previously described, which we here described as setup 3. In all of the three setups the bodies were enclosed in the interior of a plastic cone pointing downwards to significantly reduce the aerodynamic resistance (negligible air friction). In the setups described, there was coupled in the top an autonomous accelerometer, with the Z-sensor aligned in the vertical direction, the Y-sensor pointing towards north and the X-sensor pointing to East. The sensors Y and X were also at the same level on the horizontal plane. The four cylindrical magnets used in both setups 1 and 2 are constituted by neodymium ($Nd_2Fe_{14}B$) grade N35 with field $B_r = 1.17$ T, diameter diameter D = 6cm and thickness t = 2cm. All the free falls were performed in the internal ambient of our laboratory in order to reduce at maximum any possibility of lateral interference from wind. The height of the falls was approximately 1.73 m and the values of mass of the setups 1, 2 and 3 were respectively 920 g, 1000 g and 935 g, that is, they have approximately close values, remembering that the gravity acceleration of the objects must be the same one, independently of each magnitude of mass. The experimental setups were released from the top of the established height up to the collision with an damper (foam) on the ground of the laboratory. The average time of the free fall was approximately 0.50s. The autonomous accelerometer used in our experiments was the Model X6-2 built by Gulf Coast Data Concepts, which was configured with resolution 16 bits, sample rate 320Hz and zero-g at the office level, with accuracy 0.004 g to Z-sensor. Such an accelerometer with technology MEMS does not suffer any interference due to static magnetic fields. As mentioned before, the figure 1 indicates the diagram of the setup 1 and the figure 2 shows the setup 1 physically, but without the accelerometer on the top. By analyzing the shape of the devices in the figures, one can realize that possible complications to the experiment would be some initial perturbation when dropping them and their possible rotations in the fall. Due to the fast time of fall, the latter should be significantly reduced, but even with that possibility the accelerometer detects such variations by analyzing the X-sensor and Y-sensor, so that inappropriate events can be easily discarded.

In an ideal situation, an accelerometer in free fall, that is, in conditions of microgravity, must measure null acceleration by means of their three sensors: $a_z = a_y = a_x = 0$ m/s^2. Then, in theory, if there were anomalies ($a_z \neq 0, a_x \neq 0, a_y \neq 0$) in terms of acceleration during the period of microgravity, the sensors of the accelerometer will register accordingly and that is the reason for using such a device in our experiment. The measurements of the accelerometer are more visible in terms of detection of the exact condition of microgravity and they are more accurate than the measurements of the release time and end time of fall of the magnets to verify possible lower or higher acceleration when one considers as reference the usual gravity acceleration.

The figure 3 shows the graphics of the acceleration variation of one of measurements performed by the accelerometer in free fall or microgravity. The values of the acceleration in g-force are shown in the vertical axis and values of time are shown in the horizontal axis. The green curve refers to Z-sensor, the blue one refers to the Y-sensor and the red one refers to the X-sensor. The period of microgravity is shown in the graph, in which the curves are close to the horizontal axis and whose values are close to 0 g and also parallel to such an axis. Note that in the period immediately before the time of microgravity, the green curve (Z-sensor) is close to -1g, which is the value of the usual gravity acceleration.

We performed dozens of measurements of free fall with the three setups described previously and all the curves were

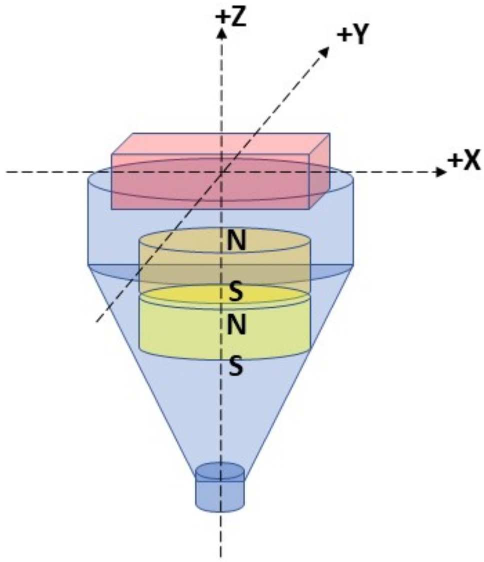

Figure 1: Diagram of the experimental setup 1. The symmetry axes of the cylindrical magnets are aligned with the symmetry axis of the cone. The magnets are under attraction with their circular faces (opposite poles) separated by a paper sheet with thickness 1mm.

systematically analyzed. In general, the ideal condition $a_z = a_y = a_x = 0$ m/s^2 did not occur in practice, although the values measured of acceleration during the microgravity were close to 0 g, but they presented some weak positive or negative value of average residual offset higher than the accelerometer offset (0.004 g).

The perturbations (mechanical oscillations, rotations, etc.) during the free fall were well visible in the systematical analysis done by considering the acceleration curves and therefore many curves were discarded. After such a filtering to obtain the valid curves, we only considered the values of acceleration hundredths of a second before the impact of the setups with the dampers (foam) to guarantee a great attenuation of any initial perturbation that occurred when the setups were released to start the free fall.

The protocol adopted to verify the existence of possible anomalies is the comparison of the average of the accelerations measured during free falls in setups 1 (magnet in attraction) and 2 (magnets in repulsion) with the average of accelerations during free falls in setups 3 (quartz crystals - non-magnetic materials). Such comparisons were made considering the Z-sensor (vertical direction). According to current theories, there should be no differences. The results are shown in table 1.

Table 1: Average of the accelerations obtained in the setup 1 (attraction), in the setup 2 (repulsion) and in the setup 3 (neutral body). In the fourth and fifth columns we see the difference between the attraction and neutral measurements and the difference between the repulsion and neutral measurements, respectively. The second line corresponds to the values of the average accelerations obtained by means of the measurements of the accelerometer.

Neutral a_n	Attraction a_a	Repulsion a_r	a_a - a_n	a_r - a_n
0.0235 g	0.0225 g	0.0246 g	-0.001 g	0.0011 g

From this table, values of force were calculated with basis on Newton's law. The variation of acceleration for the attractive magnets $\Delta a = a_a - a_n$ provides us a force 0.009 N and for the repulsive magnets $\Delta a = a_r - a_n$ we obtain -0.011 N.

By interpreting table 1, the average acceleration measured during the free fall of the attracting magnets (setup 1) was less than the average acceleration during the free fall of the neutral materials (setup 3). On the other hand, the average

Figure 2: Photo of the experimental setup 1 without the accelerometer on its top.

acceleration measured during the free fall of the magnets in repulsion (setup 2) was greater than the average acceleration during the free fall of neutral materials (setup 3). This means that the accelerometer measured a force slightly greater than that of gravity during the free fall of the attracting magnets (-0.009 N), that is, setup 1 fell at a slightly higher acceleration than setup 3 (non-magnetic or neutral materials). This also means that the accelerometer measured a slightly lower force than the gravity one during the free fall of the repulsing magnets (0.011 N), that is, setup 2 fell at a slightly lower acceleration than setup 3. One could say that the magnetic interaction of the free-falling magnets in the vertical direction with the horizontal component of the Earth's magnetic field could be responsible for the differences in measurements, but the angular variation of the dipoles is symmetrical so that the center of symmetry remains unchanged. The comparison between the averages of the acceleration measured by the Y-sensor (which pointed horizontally to the north) in the free falls of setup 1 (attraction) and in the free falls of setup 2 (repulsion) indicated a very small difference (0.0022 g), lower than the free-fall accelerometer Y-sensor offset (0.004 g).

Therefore, considering the errors and the accuracy of the measurement instrument, the anomaly was indeed verified experimentally.

We now present in the next section a theoretical proposal to explain the effect. Provided by such a theoretical proposal, we could explain our experimental results in a consistent way.

3. Theoretical Description

3.1 Analysis of the Magnetic Configuration of the Spins

The permanent ceramic magnets such as neodymium ($Nd_2Fe_{14}B$) used in our experiment are made of materials melted at high temperatures and subject to intense magnetic fields generated by external coils to magnetize the internal spins [9]. With the subsequent forced cooling (decrease in thermal energy), the material of the magnet maintains a high remaining magnetic induction B and its internal spins (magnetic dipoles) are positioned and fixed collectively and mostly in a direction parallel to that of the magnetic induction field B so that they take on a minimum potential energy.

Magnets made of neodymium are known as hard ferromagnetic magnets because they have a wide hysteresis curve [10, 11, 12, 13, 14, 15], as shown in figure 4. Therefore, they present high coerciveness for demagnetizing reverse external magnetic fields and high values of magnitude of saturation magnetic induction B_s for direct external magnetizing fields. Their internal magnetic dipoles (spins) resist in changing from their original position to both direct and reverse external magnetic fields so that magnetic induction B does not linearly follow the external magnetic field H applied to the magnet.

Figure 4 shows the hysteresis loop BH curve of the magnets used in our experiment. The horizontal red arrows above and below the curve show the width of the curve and show that the magnetic induction B remains stable before it decays with the increase in the magnitude of the applied reverse magnetic field H and also remains stable with the increase in the direct magnetic field applied H before showing a very small and asymptotic growth in saturation + B_{sat} and - B_{sat}.

This mentioned resistance of the spins is evident when two neodymium magnets are coupled as we did in our experiments

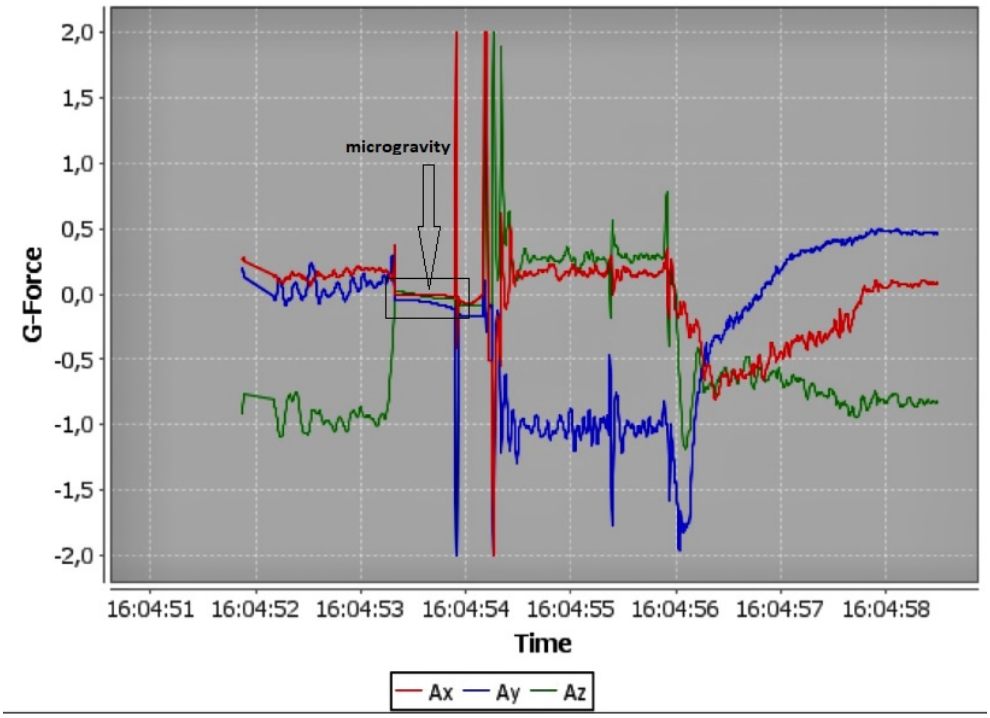

Figure 3: Curves of variation of accelerations measured by the accelerometer in all the experimental process in one of the free fall experiments.

both in attraction and in repulsion, so that an internal residual magnetic potential of greater magnitude manifests itself in comparison to the minimum magnetic potential existing when the magnets are decoupled.

In our experiment, the two coupled cylindrical magnets are identical and have a remaining magnetic induction field B_r = 1.17 T and a coerciveness H_c = 954929 A/m according to the supplier [16, 17]. In the case of two magnets coupled under repulsion, the reverse magnetic field of one affects the spins of the other, but both can only minimally demagnetize, that is, change the original magnetization of most spins because the value of coerciveness is higher than that of the remaining magnetic induction ((H_c x μ_0) > B_r). In the case of the two magnets coupled under attraction, the direct magnetic field of one affects the spins of the other, but the sum of the fields can only minimally reinforce the total magnetization because above the saturation magnetic induction B_{sat}, which is practically equal at the value of the remaining magnetic induction field B_r (1.17 T), the magnetization of the spins increases minimally. Given these two opposite situations of coerciveness and saturation, where in the first case there is a resistance of the spins to unpair and in the second case there is the opposite, that is, a resistance of the spins to pair, we assume that in these conditions there is a situation of a residual magnetic potential energy which can be associated with the effective difference of magnetic induction B_{diff}, calculated according to equation 1[18]

$$B_{diff} = \mu_0 \times H_c - B_r, \tag{1}$$

where μ_0 is the magnetic constant of the vacuum, H_c is the coercive magnetic field and B_r is the remaining magnetic induction of the magnet.

The calculated value of B_{diff} (1.2 T - 1.17 T) is then 0.03T. Considering that the gap X between the two cylindrical magnets with their symmetry centers aligned in our experiment was 1mm, then it is necessary to recalculate the intensity of the magnetic induction field B_{diff} via equation 2[19]:

$$B_{diff}(x) = \frac{B_{diff}}{2}\left[\frac{2L + x}{\sqrt{R^2 + (x + L)^2}} - \frac{x}{\sqrt{R^2 + x^2}}\right], \tag{2}$$

in which L is the length of the cylindrical magnet ($L = 2cm$) with radius $R = 3cm$. The result of the calculation is B_{diff} = 0.0284 T.

The energy density u_B associated with the magnetic induction field $B_{diff}(x)$ in J / m^3 can be calculated according to equation 3 below[20, 21], considering that the relative permeability μ_r of the gap material between magnets (cardboard)

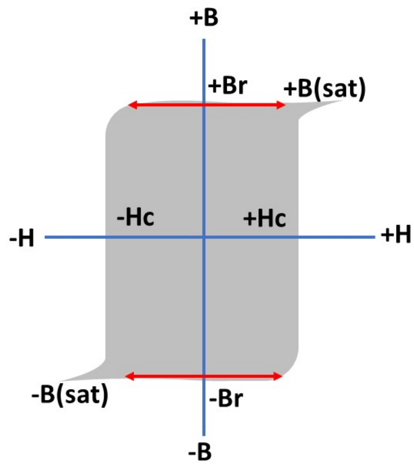

Figure 4: Curve of Hysteresis Loop B x H of the neodymium magnet used in our experiment.

not included in the equation is practically equal to 1:

$$u_B = \frac{B_{diff}^2}{2\mu_0}, \tag{3}$$

where μ_0 is the magnetic constant of the vacuum. The calculated value of u_B is 320.92 J / m^3.

The magnitude of the magnetic force F_m of resistance of the unpaired spins can be calculated by multiplying the value of the energy density u_B by the circular area S of the cylindrical magnets (S = 0.000283m^2), which results in F_m = u_B x S = 0.907 N .

This calculation is valid for magnets in attraction, but we assume that the intensity of the magnetic force Fm is the same for magnets in repulsion considering that in practice the difference is very small [22].

3.2 Analysis of the Quantum Configuration of the System

Our theoretical framework called GQE (Generalized Quantum Entanglement) considers that all particles in the Universe are in a preexisting collective quantum state, so that this allows the interaction among all the particles, even if the usual interaction via known local forces (local potentials) is negligible or non-existent, as shown in our previous works [3, 4, 23]. Such a theoretical framework leads us to a macroscopic description of our physical systems. The quantum entanglement is a non-local phenomenon and the consequence of an interaction in the past between two particles in a given time, so that after the interaction all of particles in the quantum state maintain the information from each other, even considering arbitrary huge distances [24]. So, it is naturally possible, given the quantum nature of the phenomenon, that there is a quantum interaction among all the microscopic particles and possible effects of that generalized entanglement can be observed (even for very weak magnitudes) in macroscopic physical systems. Some researchers have lately given attention to the problem, as reported in a recent work [25].

We know that there is high complexity in the quantum problem of many entangled particles, but we also suppose with basis on the so-called quantum witness[26] that some macroscopic observables can be determined from the microscopic behavior by means of a connection between the micro and macro world, so that we can successfully calculate their physical values in an easier way and relatively good accuracy, as described in the Ref. [3]. We also realized that in extreme conditions quantum entanglement macroscopic effects could be revealed and have influence on the magnitude of some macroscopic observables describing some physical systems.

Basically, the method of calculation considers that in some physical conditions the generalized entanglement among the microscopic constituents of a physical system - or the property of preexisting state of generalized quantum entanglement - can exist, manifest itself in extreme conditions and its effects could be detected in macroscopic scale and also can be classically calculated, in order to obtain the values of macroscopic observables associated to such systems.

In our experiments involving the fall of conjoined magnets, we have two systems that involve a myriad of particles: the first system is composed by the myriad of spins of the two coupled ferromagnetic magnets and the second system is the myriad of spins on the planet. The spins are subject to potential energies specific to their locations, which in the case of the coupled magnets is the joint magnetic potential. It is also considered the existence of gravitational potential energy between the systems in this case. According to the GQE theory, the spins of the magnets-planet system are also coupled, considering that they are governed by a preexisting collective joint quantum state. In order to understand the interaction between the two systems, we present the generic Hamiltonian operator[27, 28, 29, 30, 31] that rules the states indexed as n, m and g, as represented by equation 4:

$$\hat{H} = \hat{V}_n + \hat{V}_m + \hat{V}_g - \frac{h^2}{8\pi^2}\left(\sum_{n=1}^{N}\frac{1}{m_n}\nabla_n^2 + \sum_{m=1}^{N}\frac{1}{m_m}\nabla_m^2 + \sum_{n=1}^{N}\frac{1}{m_n}\nabla_{gn}^2 + \sum_{m=1}^{N}\frac{1}{m_m}\nabla_{gm}^2 + \sum_{M=1}^{N}\frac{1}{M}\nabla_{gn}^{*}\nabla_{gm} + \sum_{M=1}^{N}\frac{1}{M}\nabla_n\nabla_m\right). \quad (4)$$

In equation (4), we have the generic Hamiltonian operator of two systems of particles separated, in which they are quantically entangled. The potential energies V_n, V_m and V_g refer to the potential local and internal energy in system n, the potential local and internal energy in system m and the potential energy of gravitational interaction between systems n and m, respectively. The terms in parentheses refer respectively from left to right to the kinetic energies of systems like that of system n due to local potential energy V_n; of system m due to local potential energy V_m, of systems n and m due to their positions in the gravitational potential energy V_g and of the systems n and m in their positions due to the specific local potential energies V_n and V_m.

The energy balance between the two systems n and m is maintained by the principle of total energy conservation since they are in interaction even if there was no potential gravitational energy V_g and this corresponds to the constant value of the Hamiltonian H. So, the coupling of the particles of a system via GQE with another system causes the local action of energy from one to affect the other and vice-versa.

Considering this, specifically in our experiment, the residual potential energy of the unpaired spins of the system composed by the two coupled magnets is associated with the magnetic energy density u_B of 320.92 J / m^3 and to the magnetic force F_m (0.907 N) of resistance for both demagnetization as for the post-saturation magnetization of the unpaired spins in which also the dynamics of the spins of the other system (planet) are subject since the two systems are in mutual interaction (they are not isolated). The magnetic force F_m of resistance of the spins causes the coupled magnets to fall at an acceleration slightly different from the acceleration of gravity g. Attracting magnets fall at slightly greater acceleration than g, while repelling magnets fall at slightly less acceleration than g. Theoretically this is explained by the concept of reaction force because the magnetic field lines in the repelling magnets are divergent in order to force the resistance of the unpaired spins in omnidirectional orientation whereas in the attracting magnets the magnetic field lines are converging in order to force the resistance of the unpaired spins in the orientation of the single direction of the field. For each unpaired spin, the reaction force occurs in the opposite direction to its resistance force to the magnetic field which it is submitted to.

Figure 5 shows a diagram in which at the left side one can see the system of two magnets coupled in repulsion and free fall with their axes of symmetry aligned to the vertical axis (z); and at the right side one can see the system of two magnets coupled in attraction also in free fall and aligned to the vertical axis (z). In repulsive and free-falling magnets, a magnetic force F_m of resistance of the unpaired spins will point upwards causing them to fall at an acceleration slightly less than g, while for attraction and free fall magnets it will point downwards doing the fall to present an acceleration slightly greater than g. The experiments indicated exactly this behavior through the measurements of accelerations by the Z-sensor (vertical) emphasizing that the free fall of non-magnetic (ordinary) materials indicated a fall in an acceleration g.

Our study then indicates that the anomaly in the acceleration of coupled magnets in free fall is a purely quantum phenomenon and is due to the interaction of its internal constituents (unpaired spins) with the planet via generalized quantum entanglements (GQE). The sum of the self-energy states of the unpaired N spins must correspond to the magnitude of the magnetic energy density u_B. For a generic system of N particles, these self-energy states are calculated by the terms of kinetic energy containing the summation in parentheses multiplied by the Planck constant (h^2), as shown in equation 4.

We assume that the magnitude of the magnetic energy density uB classically calculated in the spatial volume of the two magnets as well as the magnitude of the magnetic force F_m of resistance of the unpaired spins are related to the linear dynamics where the usual Planck constant is used and we are dealing with angular dynamics[32, 33] where it is used $\hbar$ due to the fact that magnetic spins or dipoles rotate under the action of magnetic induction lines, so we must multiply these magnitudes by the constant $1/8\pi^2$ indicated in equation 4. In our previous work, this constant was widely used in the equations for determining electrical and magnetic dipolar force[4, 23].

With this, the magnitude of the magnetic force F_m of resistance of the unpaired spins multiplied by $1/8\pi^2(F_m \times 1/8\pi^2 = 0.907x1/8\pi^2)$, which gives us a value of 0.01148 N. This value is consistent with the values of force experimentally

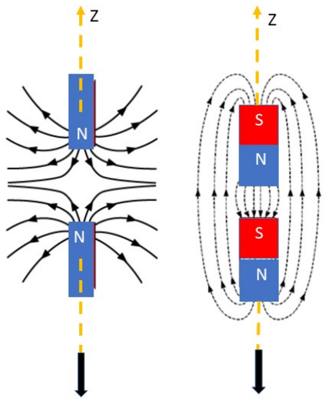

Figure 5: Magnets coupled in free fall. At left, the magnets are repulsive and at right they are attractive.

obtained shown in Table 1 so for magnets in free fall under attraction as for magnets in free fall under repulsion.

4. Conclusion

In this work, we present an experimental investigation of the existence of a decreasing (or an increasing) of the local gravity acceleration on the free fall of repulsive (attracting) conjoined magnets, in relation to the acceleration of an arbitrary ordinary body with the same mass and shape.

The motivation to perform such measurements was to implement an experimental setup with significant improvement in relation to previous cases, mainly characterized by an efficient method of collecting acceleration data from an accelerometer connected to all the setups considered.

Our experimental measurements indicated the presence of weak anomalous forces acting on the magnets setups which are responsible for the variation of the acceleration of the order of 0.01 m/s^2.

We also proposed a theoretical model for calculating the magnitude of the anomalous force responsible for the effect by considering the validity of the concepts of quantum witness and generalized quantum entanglement. By means of such a theoretical proposal we show that one can explain the effect caused by the microscopic particles on the macroscopic setups when a high magnetic field is present. In fact, the theoretical result $F_{theor} = 0.01148$ N shows good consistency with our experimental measurements, as figured out by GQE formalism.

References

[1] Boyd B. Bushman, Apparatus and method for amplifying a magnetic beam, Patent US5929732A, United States, 1999.

[2] Wordpress, Anti-Gravity Experiments. https://quantumantigravity.wordpress.com/boyd-bushman (Accessed in May 2021).

[3] E. B. Porcelli and V. S. Filho, Anomalous Effects from Dipole-Environment Quantum Entanglement, Int. J. Adv. Eng. Res. Sci., 4(1), 131-144 (2017). DOI:10.22161/ijaers.4.1.21.

[4] E. B. Porcelli and V. S. Filho, On the Possible Anomaly of Asymmetric Weight Reduction of Gyroscopes under Rotation. Trends Journal of Sciences Research, 4(1), 29-38 (2019). DOI: 10.31586/MolecularPhysics.0401.05

[5] Rob Baker, Boyd Bushman's reduction of mass gravity with opposing neodymium magnets - experiment. https://www.youtube.com/watch?v=jNTTt8ffsvg (Accessed in May 2021).

[6] Steemit, Anti-Gravity Experiment Results. https://steemit.com/science/@clearshado/anti-gravity-experiment-results (Accessed in May 2021).

[7] E. B. Porcelli, New evidences of anomalous forces involving magnetic dipoles in experiments of magnets free fall, Preprint - Experimental Findings ResearchGate, 2020, DOI: 10.13140/RG.2.2.20133.04328

[8] https://www.youtube.com/watch?v=u333pYC4b8c (Accessed in May 2021).

[9] First4Magnets, https://www.first4magnets.com/tech-centre-i61/information-and-articles-i70/neodymium-magnet-information-i82/how-are-neodymium-magnets-made-i90 (Accessed: May 2021).

[10] R. E. Hummel, Electronic Properties of Materials: An Introduction for Engineers (Berlin: Springer-Verlag, 1985).

[11] S. Chikazumi and C. D. Graham, Physics of Ferromagnetism (Oxford: Claredon, 1997).

[12] K. M. Ralls, T. H. Courtney and J. Wulff, Introduction to Materials Science and Engineering (New York: Wiley, 1976).

[13] G. Bertotti, Hysteresis in Magnetism: For Physicists, Materials Scientists, and Engineers (San Diego: Academic, 1998).

[14] Stanislav S. Naboychenko, Irina B. Murashova, Oleg D. Neikov, Handbook of Non-Ferrous Metal Powders. Technologies and Applications, Chapter 22 - Production of Rare Metal Powders, 485-537, 2005. https://doi.org/10.1016/B978-1-85617-422-0.00022-7

[15] A. G. Clegg, P. Beckley, E. C. Snelling and R. V. Major, Electrical Engineer's Reference Book, Sixteenth Edition, Chapter 8 - Magnetic Materials, Pages 8-1, 8-3-8-17, 2003.

[16] Bunting E-Magnets, https://e-magnetsuk.com/introduction-to-neodymium-magnets/grades-of-neodymium/ (Accessed: May 2021).

[17] First4Magnets, https://www.first4magnets.com/tech-centre-i61/information-and-articles-i70/neodymium-magnet-information-i82/grades-of-neodymium-magnets-i92 (Accessed: May 2021).

[18] Werner K. Schomburg, Olivier Reinertz, Johannes Sackmann, Katharina Schmitz, Equations for the approximate calculation of forces between cuboid magnets, Journal of Magnetism and Magnetic Materials, Vol. 506, 166694 (2020).

[19] IBSMagnet, https://ibsmagnet.com/fluxdensity/index.php (Accessed: May 2021)

[20] J. D. Jackson, Classical Electrodynamics (3 ed., New York: Wiley, pp. 212, 1998).

[21] R. Feynman, "The Feynman Lectures on Physics", Volume II, Chapter 15: The vector potential.

[22] Supermagnete, https://www.supermagnete.de/eng/faq/Is-the-attraction-between-magnets-as-high-as-the-repulsion (Accessed: May 2021)

[23] E. B. Porcelli and V. S. Filho, On the Anomalous Forces in High-Voltage Symmetrical Capacitors. Phys. Ess., Vol. 29, 2-9 (2016). https://doi.org/10.4006/0836-1398-29.1.002

[24] A. Zeilinger, Experiment and the foundations of quantum physics. *Rev. Mod. Phys., Vol. 71,* S288 (1999). https://doi.org/10.1103/RevModPhys.71.S288

[25] R. V. Buniy and S. D. H. Hsu, Everything is Entangled. Phys. Lett. B, Vol. 718, 233-236 (2012). https://doi.org/10.1016/j.physletb.2012.09.047

[26] M. Wieśniak, V. Vedral and C. Brukner, Magnetic Susceptibility as a Macroscopic Entanglement Witness. New J. Phys., Vol. 7, 258 1-8 (2005). https://doi.org/10.1088/1367-2630/7/1/258

[27] R. Resnick, R. Eisberg, Quantum Physics of Atoms, Molecules, Solids, Nuclei and Particles (2nd ed., John Wiley & Sons, 1985). ISBN 0-471-87373-X.

[28] P. W. Atkins, Quanta: A Handbook of Concepts (Oxford University Press, 1974). ISBN 0-19-855493-1.

[29] I. S. Grant and W. R.Phillips, Electromagnetism (Manchester Physics Series, 2nd ed., 2008). ISBN 978-0-471-92712-9.

[30] B. H. Bransden and C. J. Joachain, Physics of Atoms and Molecules (Longman, 1983). ISBN 0-582-44401-2.

[31] S. Ghosh, T. F. Rosenbaum, G. Aeppli and S. N. Coppersmith, Entangled Quantum State of Magnetic Dipoles. Nature, Vol. 425, 48-51 (2003). https://doi.org/10.1038/nature01888 .

[32] SAIPhysics, https://www.youtube.com/watch?v=xKshHdfqNF4 (Accessed May 2021).

[33] UFRJ, https://www.if.ufrj.br/ pef/aulas_seminarios/notas_de_aula/carlos_2010_1/MecanicaQuantica_parte1.pdf (Accessed May 2021).